Multiphysics CFD modeling of a free falling jet during melt-blowing slag fiberization

CFD Modeling and Simulation in Materials
Edited by: Laurentiu Nastac, Lifeng Zhang, Brian G. Thomas, Adrian Sabau, Nagy El-Kaddah, Adam C. Powell, and Hervé Combeau
TMS (The Minerals, Metals & Materials Society), 2012

MULTIPHYSICS CFD MODELING OF A FREE FALLING JET DURING MELT-BLOWING SLAG FIBERIZATION

Dimitrios I. Gerogiorgis, Dimitrios Panias and Ioannis Paspaliaris

Laboratory of Metallurgy, School of Mineral and Metallurgical Engineering
National Technical University of Athens (NTUA)
9, Heroon Polytechneiou Street, Zografou Campus; Athens, GR-15780, Greece

Keywords: Computational Fluid Dynamics (CFD), red mud, mineral wool, slag, fiberization

Abstract

Red mud fiberization is a process with remarkable potential, alleviating environmental pressure by transforming an aluminum by-product into mineral wool, thus to various marketable products. A promising mineral wool process is molten slag fiberization via an impinging air jet, which avoids mechanical wear and rotating parts. The molten slag which remains after pig iron casting flows out of a heated ladle orifice at a high temperature (1600 °C) and adjustable flowrate, and forms a free-falling vertical jet which visibly radiates its excessive heat: at a given distance, a high-velocity impinging air jet meets the vertical melt jet perpendicularly (or at an angle), inducing intensive droplet generation, subsequent fiber elongation, collection and processing.

This paper focuses on high-fidelity CFD modeling of the molten jet flow under external cooling: the model encompasses all physicochemical phenomena (melt laminar flow, radiative cooling) and considers several temperature-dependent slag transport properties in order to understand which operational degrees of freedom (manipulated variables) are useful to process optimization.

Introduction

Primary aluminium is produced from bauxite ore that which is converted into aluminium oxide, which is subsequently reduced to primary aluminium by means of electrolysis (Frank, 2005). Common industrial aluminium production practice and plants consist of two (2) distinct stages: (i) the ***production of metallurgical alumina*** (Al_2O_3) from bauxite, conducted according to the Bayer process and (ii) the ***electrolytic reduction of alumina to aluminium***, which is performed according to the Hall-Héroult process; both processes have been developed in the 19th century. Although both have been extensively investigated and optimized via technological breakthroughs (Haupin, 2001), their scientific principles and environmental issues have remained unchanged. Alternative processes, such as carbothermic aluminium production, have been the focus of long and sustained industrial interest; production-scale progress has been recently achieved via many experimental campaigns and concurrent mathematical and CFD modeling (Gerogiorgis, 2004).

In order to improve significantly the Bayer process energy and exergy efficiency and reduce substantially its environmental footprint, an arsenal of innovative technologies is required so as to transform red mud into marketable products of sustainable industrial interest (Wang, 2008). Red mud is a visible, inevitable Bayer process by-product with environmental impact, containing heavy metals (Santona, 2006) as well as oxides (Maitra, 1994) worth recovering (Kumar, 2006). The proposed process (Balomenos, 2010) uses a novel Electric Arc Furnace (EAF) technology (AMRT, 2011) to achieve the reductive smelting of red mud without laborious pre-treatment, thus producing pig iron of required purity and viscous slag suitable for mineral wool production.

This novel EAF is the Advanced Mineral Recovery Technology (AMRT) melt reduction furnace, capable of processing finely sized materials without any loss of dusty material in off-gas streams. An innovative feeder delivers the dusty raw materials directly into the electric arc zone, and a digital PLC control system minimizes electric energy losses by continuous measurement of power supply and bath impedance (AMRT, 2011). This EAF innovation is ideal for processing dust-like red mud produced by aluminium plants (mean particle size is less than 500 nm) without any pre-treatment and without substantial energy losses, providing a crucial industrial advantage.

The novel red mud treatment process which has been proposed under the auspices of ENEXAL comprises three distinct stages: feedstock preparation, reductive smelting and product handling. In the ***feedstock preparation stage*** (Stage 1) the bauxite residue is first processed in a dryer (using the countercurrent heat of the furnace off-gases) to remove the water left in the residue. The dry bauxite residue is moved to the material weighing and mixing unit, where it is blended with fluxes (CaO, SiO_2) to regulate its transport properties, and coke (C) fines towards reduction. In the ***reductive smelting stage*** (Stage 2), the mixture is fed automatically via the electronically controlled AMRT Furnace Feeding Unit to the bowl of the AMRT Furnace, where a melt of 1590 °C-1610 °C is sustained throughout the reductive smelting process (3-5 hours per batch). All off-gases generated in the AMRT Furnace (as soon as they have passed through the dryer) are filtered in an adjacent baghouse and subsequently discharged (purified) to the atmosphere. Upon completion, two immiscible liquid phases (molten slag and pig iron) remain in the furnace. In the ***product handling stage*** (Stage 3), the two phases are separated via sequential decantation (by tilting the furnace bowl on its horizontal axis), due to a considerably high density difference. The lighter slag phase is channeled into a fiberization unit and finely dispersed to mineral wool, motivating a multiscale technical problem which forms the exclusive focus of the present paper. The heavier metal phase is poured into refractory moulds and solidifies, producing pig-iron slabs.

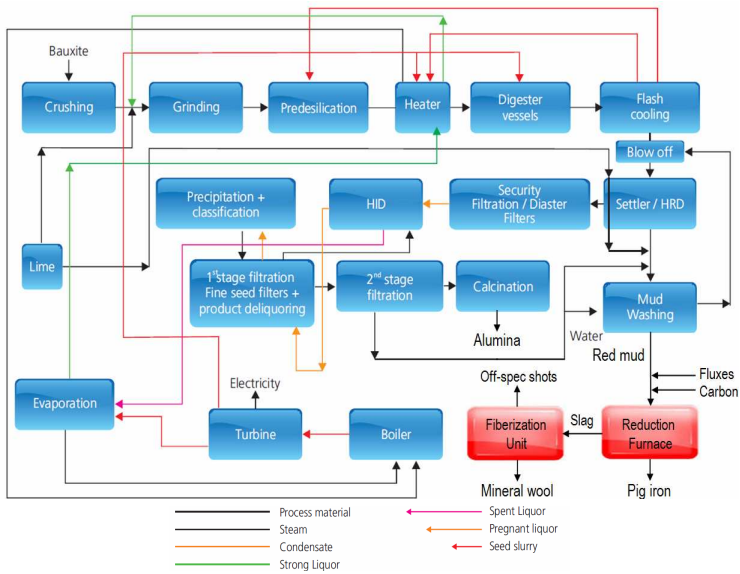

Figure 1. Process block diagram towards sustainable molten slag fiberization of red mud after alumina production.

Fiberization and Mathematical Modeling Strategy

A schematic presentation of the fiberization process via impinging gas jet is presented in Fig. 2a. The molten slag flows over a system of adjustable channels and falls as a vertical liquid stream. At the impingement point, the vertical slag stream has its minimal diameter and is subjected to strong shear forces which induce jet instability and breakup in the high-shear fiberization zone. Melt droplets (briefly connected by surface tension and viscous forces while nascent) are drawn out of the slag stream due to the propagation of microscopic instabilities on its external surface. The high-speed horizontal air jet transfers momentum to nascent fibers which follow parabolic trajectories while simultaneously undergoing cooling and elongation: as gravity prevails, cylindrical mineral wool fibers fly into a collection chamber and thus form a mineral wool layer. Off-spec product (spherical "shots") either falls very close to the fiberization zone, or is trapped and inevitably solidified within the cooled material as it accumulates into the collection chamber.

The mathematical modeling strategy which is proposed in order to facilitate the study of molten slag fiberization is based on the concept of zone decomposition: as the process encompasses a variety of mass, heat and momentum transport phenomena, one can define 3 distinct zones, in each of which different phenomena prevail and different questions must be answered (Fig. 2b).

Zone 1: Molten slag bulk flow. The first zone of the fiberization process is the vertical slag stream emanating from the heated slag ladle: volumetric flow is controllable via ladle tilt angle. The prevalent phenomenon is macroscopic free surface laminar flow, also characterized by a nonisothermal temperature field (molten slag jet cooling due to forced convection and radiation). Both momentum and heat problems yield homogeneous solution fields with high observability.

Zone 2: Mineral fiber generation. The core zone of the fiberization process is the small volume within which the vertical slag stream disintegrates upon meeting the horizontal impinging air jet. The main phenomenon is microscopic molten slag fiber generation, characterized satisfactorily by the approximation of an isothermal temperature field, due to the very low residence times. The momentum problem yields an inhomogeneous two-phase field with rather low observability.

Zone 3: Dispersed flow of fibers. The final zone of the fiberization process is an extended cone produced by all isolated fibre trajectory curves emanating from the foregoing fiberization zone. This is a macroscopic dispersed flow zone, characterized by a nonisothermal temperature field with sharp gradients between and inside each fiber, due to their intensive cooling and elongation. The momentum problem yields a dynamic inhomogeneous field with moderate observability.

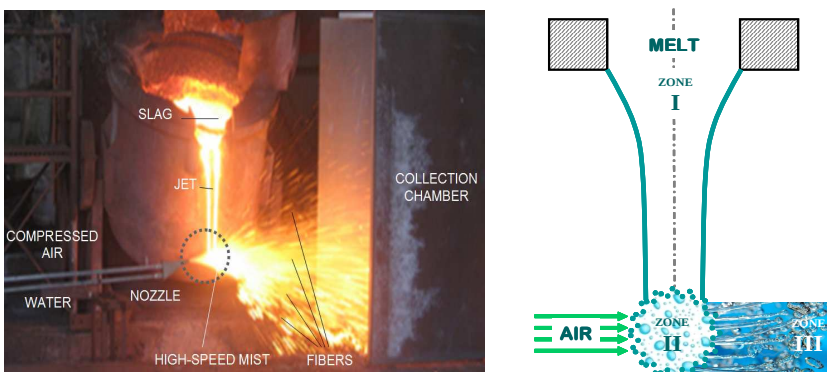

Figure 2. (a) Molten slag fiberization demonstration unit, **(b)** Mathematical modeling strategy and zone definition.

Thermophysical Property Modeling and Operation Parameters

An extensive literature survey has led to numerous papers proposing elaborate thermophysical property models of silicate melts and validating most successfully against experimental data. Because molten slag properties (esp. density, viscosity and surface tension) are theoretically expected (and experientially known) to affect process operation (hence, product quality) to a significant extent, a computational investigation of property models is very important in order to: (a) a priori delineate property variation bounds for the given temperature range (1300-1800 °C), (b) comparatively validate the best of these models against pilot plant data as soon as possible, (c) calculate dimensionless numbers and their bounds and use them as plant diagnostic metrics, (d) correlate online property data with operation regimes during upcoming pilot plant campaigns.

Density (ρ). The density correlation by Širok et al. (2005) has been employed to compute slag density values for representative compositions (Balomenos, 2010) in the 1300-1800 °C range. Density is determined to vary between $\mathbf{2.589 \cdot 10^3\ kg.m^{-3}}$ (1800 °C) and $\mathbf{2.755 \cdot 10^3\ kg.m^{-3}}$ (1300 °C).

Viscosity (μ). The viscosity correlation by Browning (2003) has been used so as to calculate slag viscosity values for the same representative compositions in the same 1300-1800 °C range. Viscosity is determined to vary greatly, between **0.024 Pa.s** (1800 °C) and **3.046 Pa.s** (1300 °C).

Surface tension (σ). Due to the scarcity of temperature-dependent surface tension correlations, we decided to compile all surface tension measurements for adequately similar silicate slags. Based on a literature survey (Magidson et al., 2009; Arutyunyan et al., 2010) we have determined that slag surface tension varies between $\mathbf{0.368\ N.m^{-1}}$ and $\mathbf{0.510\ N.m^{-1}}$, depending on composition.

Operation parameters (d, U). On the basis of video recordings of fiberization experiments, qualitative visual observations can be made about key dimensions and operation parameters. Slag jet diameter and velocity are estimated between **0.05-0.20 m** and $\mathbf{0.05\text{-}0.20\ m.s^{-1}}$, while slag drop diameter and velocity are estimated between **0.001-0.01 m** and $\mathbf{0.5\text{-}2.0\ m.s^{-1}}$, respectively.

Thermophysical properties as a function of temperature for CFD study are presented in Figure 3.

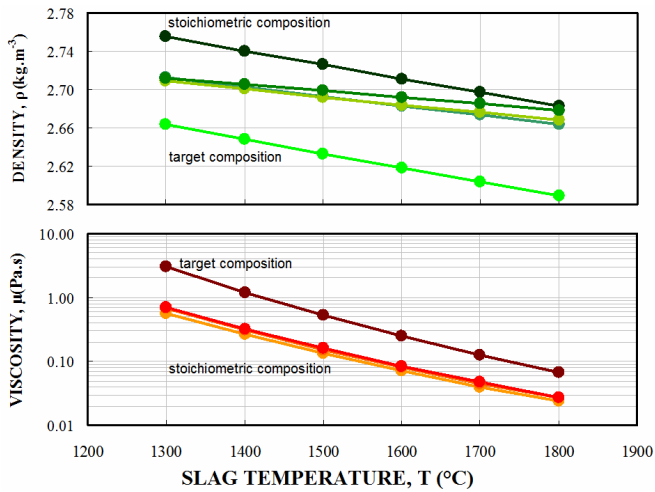

Figure 3. (a) Density, **(b)** Viscosity of molten red mud slags of variable composition as a function of temperature.

Computational Fluid Dynamics (CFD) Results and Discussion

The problem of free-surface homogeneous nonisothermal laminar flow under radiative cooling was first been tackled by Epikhin et al. (1981), with a rigorous mathematical (PDE) formulation but without adequate computational exploration of key dimensionless number (Re, Ca) effects. Conversely, Georgiou et al. (1988) and Adachi et a. (1990) published detailed numerical studies of vertical laminar Newtonian liquid jets, but without considering any simultaneous heat effects. Leroux et al. (1997) proved that the free surface boundary is reliably captured by quartic curves, while Novitskii and Efremov (2006) provided mineral fiber size phenomenological correlations. Melt-blowing slag fiberization is studied rigorously via COMSOL Multiphysics®, considering unperturbed laminar flow and radiative cooling in an axisymmetric unstructured grid (Figure 4).

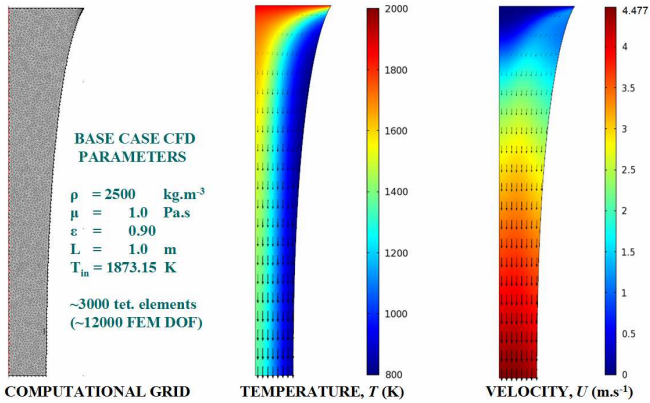

Figure 4. Axisymmetric unstructured grid and indicative solution profiles for the nonisothermal flow problem.

The homogeneous, nonisothermal laminar molten slag stream emanates from the pot orifice and gradually experiences diameter reduction and momentum gain due to gravitational acceleration. Intense radiative cooling heat losses are evident on the free surface throughout the stream height. The stream bottom sustains enormous temperature gradients (> 400 °C) while slag enters Zone 2.

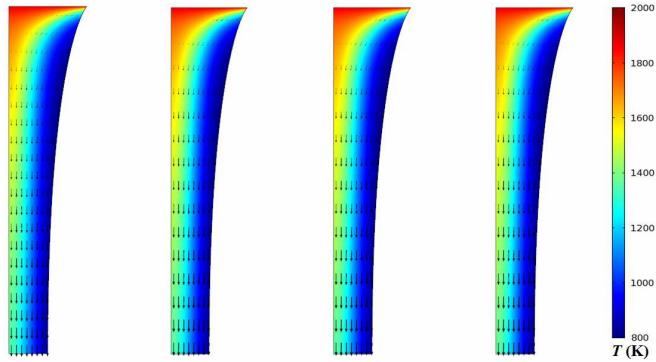

Figure 5. Vertical stream temperature and flow field as a function of density (ρ = 2500, 2600, 2700, 2800 kg.m^{-3}).

Figures 5-9 illustrate the temperature field variation due to 5 sensitivity variables (ρ, μ, ε, T, L).

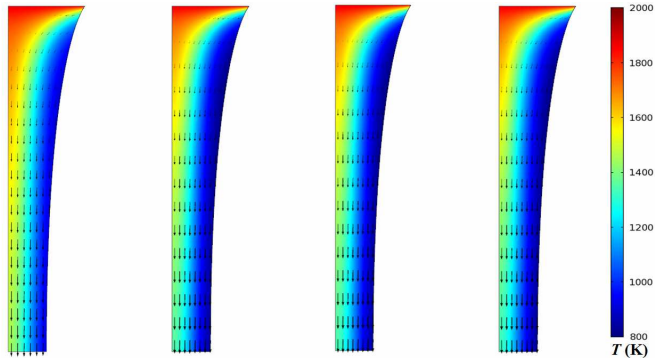

Figure 6. Vertical stream temperature and flow field as a function of molten slag viscosity (μ = 0.5, 1.0, 2.0, 3.0 Pa.s).

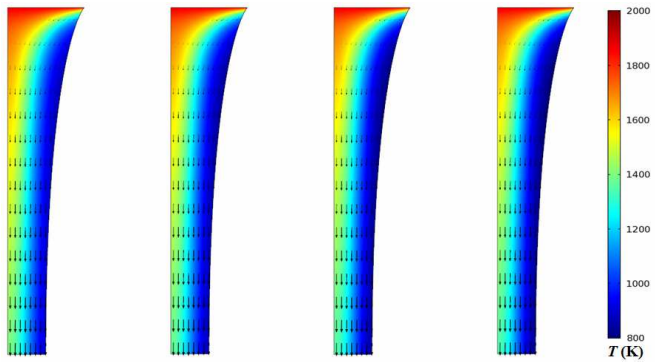

Figure 7. Vertical stream temperature and flow field as a function of molten slag emissivity (ε = 0.7, 0.8, 0.9, 0.95).

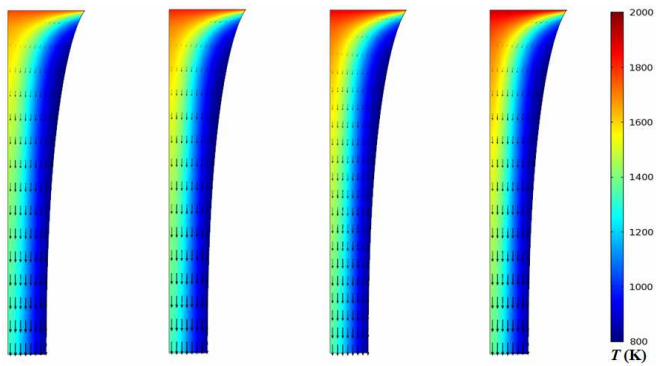

Figure 8. Vertical stream temperature and flow field as a function of pot temperature (T = 1500, 1550, 1600, 1650 °C).

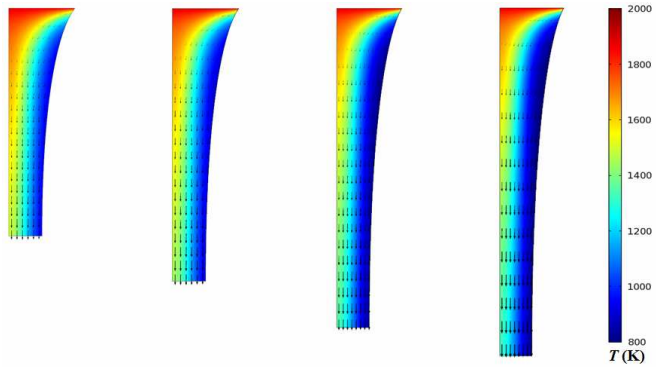

Figure 9. Vertical slag stream temperature and flow field as a function of impingement point (L=0.6, 0.8, 1.0, 1.2 m).

A sensitivity analysis of vertical slag stream temperature and flow profiles has been conducted in order to probe the heat effect (if any) of key macroscopic variables on slag as it enters Zone 2. The foregoing series of temperature distributions summarize the sensitivity analysis undertaken and illustrate that, while for some parameters CFD results appear almost indistinguishable, the quadratic and quartic nonlinearity of transport properties (viscosity and emissivity, respectively) produce clear (often accentuated) temperature gradients at the bottom of the molten slag stream. Temperature and its gradients therein are indeed vital for fiberization: a lower than appropriate temperature results in rapid slag solidification, thus hindering efficient nascent fiber generation. A higher than appropriate temperature may conversely result in excessive fine droplet generation and subsequent breakup, thus inducing the highly undesirable effect of molten slag atomization. Sharp exit temperature gradients also have more complicated effects on fiber size distribution, as the impinging gas jet meets a cooler, more cohesive skin and then a warmer, less cohesive core. Figure 10 summarizes the effect of all parameters on minimum and maximum exit temperatures of the molten slag stream, for each set of points entirely capturing the respective variation range.

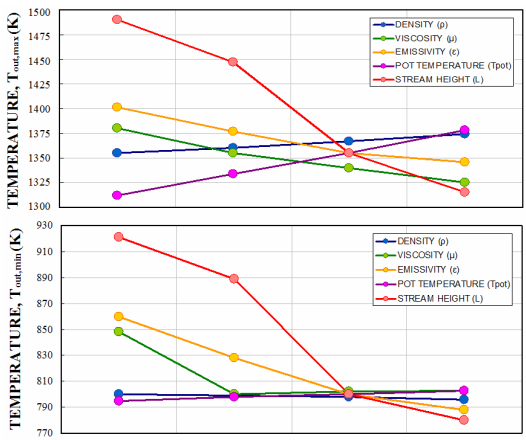

Figure 10. (a) Maximum and **(b)** minimum stream bottom temperature with respect to sensitivity analysis variables.

Conclusions

Molten inorganic slag fiberization has a strong industrial potential which requires detailed study: in particular, melt-blowing plants can surpass the widely established melt-spinning technologies. A mathematical modeling strategy for mineral slag fiberization has been outlined, on the basis of the concept that multiphase mass and heat flow can be studied efficiently in 3 distinct zones. Multiphase mass, heat and flow CFD modeling is required in order to understand how externally manipulated process parameters affect state variable profiles and thereby fiber size and quality. Thermophysical properties of slags (density, viscosity, surface tension) have been investigated in detail, and the best temperature-dependent correlations have been used to obtain reliable bounds. The nonisothermal slag flow problem has been solved employing COMSOL Multiphysics®, and axisymmetric temperature and flow fields have been obtained as a function of 5 key parameters. A sensitivity CFD analysis of minimum and maximum stream bottom temperatures has indicated that (in contrast to slag density) viscosity and emissivity are pivotal toward efficient fiberization, implying that provisions for accurate field measurements thereof are necessary in all pilot plants. The vertical distance between pot outlet and jet impingement point (the molten slag stream size) has a confirmed paramount importance, constituting the most efficient process control variable. Flexibly varying outlet diameter and stream height is thus a necessity for novel fiberization units. Continuing and integrating zone flow CFD studies is vital towards efficient pilot plant operation.

Acknowledgements

The authors gratefully acknowledge funding by the EU Seventh Framework Programme (FP7/2007-2013) under Grant Agreement No. ENER/FP7EN/249710/ENEXAL (Website: www.labmet.ntua.gr/ENEXAL).

References

1. Adachi, K., Tagashira, K., Banba, Y., Tatsumi, H., Machida, H., Yoshioka, N., Steady laminar round jets of a viscous liquid falling vertically in the atmosphere, *AIChE J.* **36**(5): 738-745 (1990).
2. AMRT-Advanced Mineral Recovery Technologies, http://amrt.co.uk/index.html (2011).
3. Arutyunyan, N.A., Zaitsev, A.I., Shaposhnikov, N.G., Surface tension of $CaO\text{-}Al_2O_3$, $CaO\text{-}SiO_2$ and $CaO\text{-}Al_2O_3\text{-}SiO_2$ melts, *Rus. J. Phys. Chem. A* **84**(1): 7-12 (2010).
4. Balomenos, E., *Thermodynamic study of red mud treatment*, ENEXAL Technical Report, NTUA (2010).
5. Browning, G.J., Bryant, G.W., Hurst, H.J., Lucas, J.A., Wall, T.F., An empirical method for the prediction of coal ash slag viscosity, *Energy & Fuels* **17**(3): 731-737 (2003).
6. Epikhin, V.E., Kulago, A.E., Shkadov, V.Y., Influence of convection and thermal radiation on the cooling of a vertically incident jet of melt, *J. Eng. Phys. Thermophys.* **41**(4): 1091-1099 (1981).
7. Frank W.B. et al., *Aluminium*, Wiley-VCH Verlag GmbH & Co (2005).
8. Georgiou, G.C., Papanastasiou, T.C., Wilkes, J.O., Laminar Newtonian jets at high Reynolds number and high surface tension, *AIChE J.* **34**(9): 1559-1562 (1988).
9. Gerogiorgis, D.I., *Multiscale Process and CFD Modeling for Distributed Chemical Process Systems: Application to Carbothermic Aluminium Production*, PhD Thesis, Carnegie Mellon University (2004).
10. Haupin, W., Aluminum production and refining, in: Buschow K.H. et al. (editors), *Encyclopedia of Materials: Science and Technology*, pp. 132-141, Elsevier, Amsterdam (2001).
11. Leroux, S., Dumouchel, C., Ledoux, M., The break-up length of laminar cylindrical liquid jets. Modification of Weber's theory, *Int. J. Fluid Mech. Res.* **24**(1-3): 428-438 (1997).
12. Magidson, I.A., Basov, A.V., Smirnov, N.A., Surface tension of $CaO\text{-}Al_2O_3\text{-}SiO_2$ oxide melts, *Rus. Metal. (Metally)* **2009**(7): 631-635 (2009).
13. Novitskii, A.G., Efremov, M.V., A study of the fiber blowing process in the production of mineral wool, *Refract. Ind. Ceram.* **47**(2): 121-124 (2006).
14. Širok, B., Blagojević, B., Bullen, P., Dimovski, D., Density and viscosity of the silicate melts for the production of the mineral wool fibres, *Int. J. Microstructure Mat. Prop.* **1**(1): 61-73 (2005).
15. Wang S. et al., Novel applications of red mud as coagulant, adsorbent and catalyst for environmentally benign processes, *Chemosphere* **72**: 1621–1635 (2008).